

PAPER • OPEN ACCESS

## Simulation of vehicle's lateral dynamics using nonlinear model with real inputs

To cite this article: D Miloradovic *et al* 2019 *IOP Conf. Ser.: Mater. Sci. Eng.* **659** 012060

View the [article online](#) for updates and enhancements.

### You may also like

- [Motion law and density influence of a submersible aerial vehicle in the water-exit process](#)  
Qiang Zhang, Jun-hua Hu, Jin-fu Feng et al.
- [Establishment, maintenance, and re-establishment of the safe and efficient steady-following state](#)  
Deng Pan, , Ying-Ping Zheng et al.
- [A new continuum model with driver's continuous sensory memory and preceding vehicle's taillight](#)  
Cong Zhai and Weitao Wu



**HONOLULU, HI**  
October 6-11, 2024

*Joint International Meeting of*  
The Electrochemical Society of Japan (ECSJ)  
The Korean Electrochemical Society (KECS)  
The Electrochemical Society (ECS)



Early Registration Deadline:  
**September 3, 2024**

**MAKE YOUR PLANS NOW!**



# Simulation of vehicle's lateral dynamics using nonlinear model with real inputs

**D Miloradović<sup>1</sup>, J Glišović<sup>1</sup>, N Stojanović<sup>1</sup> and I Grujić<sup>1</sup>**

<sup>1</sup> University of Kragujevac, Faculty of Engineering, 6 Sestre Janjić Str., 34000 Kragujevac, Serbia

E-mail: nejia@kg.ac.rs

**Abstract.** Basic understanding of vehicle's lateral dynamics may be achieved by using relatively simple mathematical-mechanical models. However, these models are often linearized and do not take into account nonlinear phenomena in vehicle's lateral dynamics and highly nonstationary nature of vehicle's vibrations in real driving conditions. One form of nonlinear nonstationary model of vehicle's lateral dynamics is developed in this paper. Simulations were conducted using experimentally recorded values of the steering wheel angle for generation of the front wheels steer angle, and vehicle longitudinal velocity as inputs to the model. Results of simulations of vehicle angular vibrations around the vertical axis, angular body side slip vibrations, tire slip angles, vehicle lateral acceleration wheel forces and inertial force are presented and discussed. Finally, conclusions regarding possible further use of the developed model were drawn.

## 1. Introduction

Simple vehicle dynamics models that specifically represent its lateral, longitudinal and vertical dynamics have been established for basic understanding of its dynamic behaviour. These types of models are commonly used with linearized form of mechanical-mathematical equations, which is desirable in design of stability controllers, active suspension systems and other driver's assistance systems.

Required complexity of the vehicle model depends on its concrete application. For example, for research of the vehicle handling characteristics during its planar motion, simple models that include only degrees of freedom in the plane are sufficient. Two-axle models with one or two tracks are used in the analysis of vehicle stability. Single-track model is used for the analysis of vehicle road holding ability or the analysis of vehicle roll. In addition to single-track models, there are many other models modelling the vehicle lateral motion with different levels of complexity. These models are usually integrated dynamical models that observe vehicle longitudinal and lateral velocity simultaneously, by observing the tire slip angle.

The usual models for vehicle lateral dynamics are [1]:

- two-axle models with single track,
- two-axle models with two tracks - planar models,
- single-axle models with two tracks and
- spatial models.

Lateral dynamics of vehicles has been studied since 1950's [2]. However, Rieker & Schunk proposed a very often used single-track model, frequently referred to as "Rieker-Schunk single-track



model”, back in 1940. It involved some simplifications which did not significantly influence the basic analysis of vehicle behaviour for lateral accelerations up to 0.4g [3], but which notably reduced a number of degrees of freedom of the system. Years later, this model was used as an ESP input in practice [4].

Analysis of simple single-track models can explain a large part of dynamic behaviour during handling of the vehicle, especially during stationary ride [5-8]. This enables faster testing and analysis of vehicle behaviour during ride and easy translation of the models to the language of simulation programs.

Although they contain certain reductions, the single-track models of vehicle lateral dynamics are nowadays used in the design of steering system control units. However, due to their nature, these models do not take into account the redistribution of weight in the lateral direction, nor the angular oscillations of the vehicle around the longitudinal axis. That is why the spatial two-track models of the vehicle are used instead, which observe the behaviour of each tire separately and which may be used in the design of the electronic stability control systems of the vehicle. The two-track models of vehicle's lateral dynamics may have a complex structure and they demand modelling using modern computer programs.

The linear single-track models contain simplifications regarding the assumption of small angles and linear dependence between wheel forces and slip angle. In addition, they do not take into account highly nonstationary nature of vehicle vibrations induced by variable vehicle velocity or road roughness [9]. Considering the previous limitations, a nonlinear nonstationary single-track model of the vehicle was used for simulation of vehicle's lateral dynamics in this paper. The used model considered larger values of body slip angles and tire slip angles, in which case the linearized equations of motion were no longer valid. In addition, the selected model considered longitudinal, lateral and yaw motion of the vehicle, under the assumption that the vehicle travels over even road and that there was negligible lateral weight shift and roll of the vehicle.

## 2. Nonlinear single-track model of the vehicle

Linear equations of motion of the vehicle single-track model do not adequately describe the vehicle's motion when large steering angles or body slip angles larger than  $10^\circ$  occur. That is why nonlinear equations describing the vehicle's lateral dynamics should be used. The nonlinear model of the vehicle lateral dynamics adopted in this research is shown in figure 1, where:

- $m$  is vehicle mass,
- $j_x, j_y$  are longitudinal and lateral acceleration of the vehicle, respectively,
- $F_{ix}, F_{iy}$  are longitudinal and lateral components of the inertial force, respectively,
- $Y_1, Y_2$  are lateral forces acting on the front and the rear wheels, respectively,
- $J_z$  is moment of inertia of mass  $m$  about vertical gravity axis,
- $a, b$  are distances between the front and the rear axle and the centre of gravity, T, respectively,
- $l$  is vehicle's wheel base,
- $r$  is turn radius,
- $v$  is vehicle velocity,
- $v_1, v_2$  are the front and the rear wheel velocities, respectively,
- $\varphi$  is ride angle (angle between vehicle velocity direction and reference axis direction ),
- $\varepsilon$  is angle of rotation of vehicle body about vertical axis (angle between longitudinal vehicle axis direction and reference axis direction, yaw angle),
- $\theta$  - body side slip angle (angle between velocity direction and longitudinal vehicle axis direction),
- $\lambda_1, \lambda_2$  are steering angles of the front and the rear wheels, respectively,

- $\delta_1, \delta_2$  are tire slip angles of the front and the rear wheels, respectively.

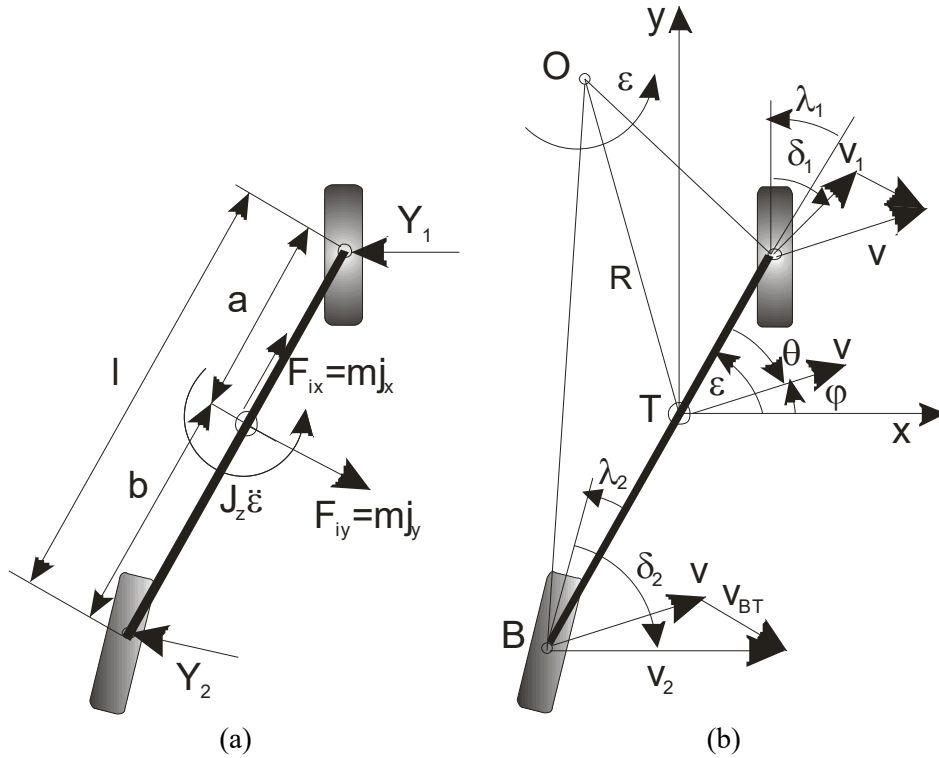


**Figure 1.** Nonlinear single-track model of the vehicle: (a) forces acting on vehicle, (b) definition of the observed angles and velocity directions.

In simplified models, tire lateral forces,  $Y_1, Y_2$ , are perpendicular to vehicle's longitudinal axis. In reality, these forces act perpendicular to wheel longitudinal axis, figure 1 (a), and this must be taken into account when writing the equations of motion. Unlike the linearized equations of motion of a single-track vehicle model, the equations of motion of nonlinear model contain projections of forces in the direction of longitudinal axis of the vehicle, which, in this case, appear as deceleration forces acting on the centre of gravity in longitudinal vehicle axis,  $x_v$ :

$$m \cdot j_{x_v} = -Y_1 \cdot \sin \lambda_1 - Y_2 \cdot \sin \lambda_2 \quad (1)$$

and in lateral vehicle axis,  $y_v$ :

$$m \cdot j_{y_v} = Y_1 \cdot \cos \lambda_1 + Y_2 \cdot \cos \lambda_2. \quad (2)$$

Acceleration vector of some point has its tangential and normal component:

$$\vec{a} = \dot{v} \cdot \vec{e}_t + \frac{v^2}{R} \cdot \vec{e}_n \quad (3)$$

According to figure 1, tangential ( $\vec{e}_t$ ) and normal ( $\vec{e}_n$ ) component of the unity vector are obtained in the following manner:

$$\vec{e}_t = \begin{pmatrix} \cos \theta \\ -\sin \theta \end{pmatrix}, \quad (4)$$

$$\vec{e}_n = \begin{pmatrix} \sin \theta \\ \cos \theta \end{pmatrix}. \quad (5)$$

Now, acceleration components of vehicle mass in direction of  $x_v$ -axis and  $y_v$ -axis are:

$$j_{x_v} = \dot{v} \cdot \cos \theta + \frac{v^2}{R} \cdot \sin \theta, \quad (6)$$

$$j_{y_v} = -\dot{v} \cdot \sin \theta + \frac{v^2}{R} \cdot \cos \theta. \quad (7)$$

Considering that:

$$\frac{v^2}{R} = \frac{v}{R} \cdot \dot{\varphi} \cdot R = v \cdot (\dot{\varepsilon} - \dot{\theta}), \quad (8)$$

the following relations are obtained:

$$j_{x_v} = \dot{v} \cdot \cos \theta + v \cdot (\dot{\varepsilon} - \dot{\theta}) \cdot \sin \theta, \quad (9)$$

$$j_{y_v} = -\dot{v} \cdot \sin \theta + v \cdot (\dot{\varepsilon} - \dot{\theta}) \cdot \cos \theta. \quad (10)$$

By substituting equations (9) and (10) into equations (1) and (2), respectively, the following equations are obtained:

$$m \cdot [\dot{v} \cdot \cos \theta + v \cdot (\dot{\varepsilon} - \dot{\theta}) \cdot \sin \theta] = -Y_1 \cdot \sin \lambda_1 - Y_2 \cdot \sin \lambda_2, \quad (11)$$

$$m \cdot [-\dot{v} \cdot \sin \theta + v \cdot (\dot{\varepsilon} - \dot{\theta}) \cdot \cos \theta] = Y_1 \cdot \cos \lambda_1 + Y_2 \cdot \cos \lambda_2 \quad (12)$$

By expressing the acceleration  $\dot{v}$  from equations (11) and (12) and equating the two obtained relations, the following relations are gained:

$$\dot{v} = -\frac{Y_1 \cdot \sin \lambda_1 + Y_2 \cdot \sin \lambda_2}{m \cdot \cos \theta} - v \cdot (\dot{\varepsilon} - \dot{\theta}) \cdot \frac{\sin \theta}{\cos \theta} = -\frac{Y_1 \cdot \cos \lambda_1 + Y_2 \cdot \cos \lambda_2}{m \cdot \sin \theta} + v \cdot (\dot{\varepsilon} - \dot{\theta}) \cdot \frac{\cos \theta}{\sin \theta}, \quad (13)$$

or

$$\frac{Y_1 \cdot \cos \lambda_1 + Y_2 \cdot \cos \lambda_2}{m \cdot \sin \theta} - \frac{Y_1 \cdot \sin \lambda_1 + Y_2 \cdot \sin \lambda_2}{m \cdot \cos \theta} = v \cdot (\dot{\varepsilon} - \dot{\theta}) \cdot \left( \frac{\cos \theta}{\sin \theta} + \frac{\sin \theta}{\cos \theta} \right). \quad (14)$$

By multiplying the first and the second term of the left side of equation (14) with  $\frac{\cos \theta}{\cos \theta}$  and  $\frac{\sin \theta}{\sin \theta}$ , respectively, and applying the sine theorem to the right side of the same equation, the following is obtained:

$$\frac{(Y_1 \cdot \cos \lambda_1 + Y_2 \cdot \cos \lambda_2) \cdot \cos \theta}{m \cdot \sin \theta \cdot \cos \theta} - \frac{(Y_1 \cdot \sin \lambda_1 + Y_2 \cdot \sin \lambda_2) \cdot \sin \theta}{m \cdot \cos \theta \cdot \sin \theta} = v \cdot (\dot{\varepsilon} - \dot{\theta}) \cdot \frac{1}{\sin \theta \cdot \cos \theta}, \quad (15)$$

or

$$\frac{Y_1 \cdot (\cos \lambda_1 \cdot \cos \theta - \sin \lambda_1 \cdot \sin \theta)}{m \cdot \sin \theta \cdot \cos \theta} + \frac{Y_2 \cdot (\cos \lambda_2 \cdot \cos \theta - \sin \lambda_2 \cdot \sin \theta)}{m \cdot \sin \theta \cdot \cos \theta} = \frac{v \cdot (\dot{\varepsilon} - \dot{\theta})}{\sin \theta \cdot \cos \theta}. \quad (16)$$

By applying the angle addition formula  $\cos(\alpha + \beta) = \cos \alpha \cdot \cos \beta - \sin \alpha \cdot \sin \beta$  to equation (16) and then expressing  $\dot{\theta}$  from the same equation, a differential equation for body slip angle is formed:

$$\dot{\theta} = \dot{\varepsilon} - \frac{1}{m \cdot v} \cdot [Y_1 \cdot \cos(\lambda_1 + \theta) + Y_2 \cdot \cos(\lambda_2 + \theta)]. \quad (17)$$

Equation of equilibrium of moments for the adopted vehicle model is:

$$J_z \cdot \ddot{\varepsilon} = Y_1 \cdot a \cdot \cos \lambda_1 - Y_2 \cdot b \cdot \cos \lambda_2. \quad (18)$$

Substituting known relations between lateral forces and tire slip angles [1, 3]:

$$\begin{aligned} Y_1 &= k_1 \cdot \delta_1, \\ Y_2 &= k_2 \cdot \delta_2, \end{aligned} \quad (19)$$

(where  $k_1, k_2$  are the front and the rear lateral force coefficients, respectively) and definitions of tire side slip angles, according to figure 1:

$$\begin{aligned}\delta_1 &= \lambda_1 - \arctg\left(\frac{a \cdot \dot{\varepsilon} - v \cdot \sin \theta}{v \cdot \cos \theta}\right), \\ \delta_2 &= \lambda_2 + \arctg\left(\frac{b \cdot \dot{\varepsilon} + v \cdot \sin \theta}{v \cdot \cos \theta}\right).\end{aligned}\quad (20)$$

into equations (17) and (18), the following differential equations of motion are obtained:

$$\dot{\theta} = \dot{\varepsilon} - \frac{1}{m \cdot v} \left\{ k_1 \cdot \left[ \lambda_1 - \arctg\left(\frac{a \cdot \dot{\varepsilon} - v \cdot \sin \theta}{v \cdot \cos \theta}\right) \right] \cdot \cos(\lambda_1 + \theta) + k_2 \cdot \left[ \lambda_2 + \arctg\left(\frac{b \cdot \dot{\varepsilon} + v \cdot \sin \theta}{v \cdot \cos \theta}\right) \right] \cdot \cos(\lambda_2 + \theta) \right\}, \quad (21)$$

$$\ddot{\varepsilon} = \frac{1}{J_z} \cdot \left\{ k_1 \cdot \left[ \lambda_1 - \arctg\left(\frac{a \cdot \dot{\varepsilon} - v \cdot \sin \theta}{v \cdot \cos \theta}\right) \right] \cdot a \cdot \cos \lambda_1 - k_2 \cdot \left[ \lambda_2 + \arctg\left(\frac{b \cdot \dot{\varepsilon} + v \cdot \sin \theta}{v \cdot \cos \theta}\right) \right] \cdot b \cdot \cos \lambda_2 \right\}. \quad (22)$$

Equations (21) and (22) describe mutual relations between different parameters of motion in nonlinear single-track model of lateral dynamics and parameters of vehicle and tires.

When only front wheels are steered ( $\lambda_2 = 0$ ), equations (21) and (22) become:

$$\dot{\theta} = \dot{\varepsilon} - \frac{1}{m \cdot v} \left\{ k_1 \cdot \left[ \lambda_1 - \arctg\left(\frac{a \cdot \dot{\varepsilon} - v \cdot \sin \theta}{v \cdot \cos \theta}\right) \right] \cdot \cos(\lambda_1 + \theta) + k_2 \cdot \arctg\left(\frac{b \cdot \dot{\varepsilon} + v \cdot \sin \theta}{v \cdot \cos \theta}\right) \cdot \cos \theta \right\}, \quad (23)$$

$$\ddot{\varepsilon} = \frac{1}{J_z} \left\{ k_1 \cdot \left[ \lambda_1 - \arctg\left(\frac{a \cdot \dot{\varepsilon} - v \cdot \sin \theta}{v \cdot \cos \theta}\right) \right] \cdot a \cdot \cos \lambda_1 - k_2 \cdot \arctg\left(\frac{b \cdot \dot{\varepsilon} + v \cdot \sin \theta}{v \cdot \cos \theta}\right) \cdot b \right\}. \quad (24)$$

Equations (23) and (24) were the basis for development of MATLAB/Simulink program for simulation of lateral vehicle dynamics in case of nonlinear nonstationary vehicle model with real inputs, figure 2.

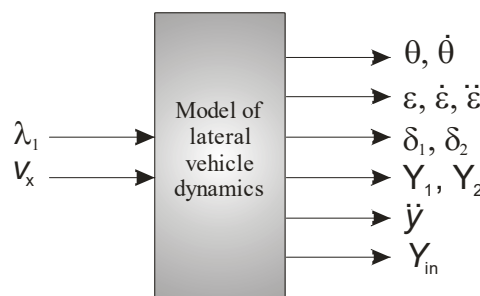


**Figure 2.** Inputs and outputs of the model of lateral vehicle dynamics.

The used mathematical model introduces the coupling between lateral and longitudinal vehicle dynamics through measured longitudinal vehicle velocity component,  $v_x$ . Namely, directly measured longitudinal component of vehicle velocity,  $v_x$ , and the front wheel steering angle,  $\lambda_1$ , determined from the measured steering wheel angle,  $\beta_v$ , were used as real inputs of the mathematical model.

Measured longitudinal component of vehicle velocity,  $v_x$ , is related to vehicle velocity,  $v$ , and body side slip angle,  $\theta$ , in the following manner:

$$v_x = v \cdot \cos \theta. \quad (25)$$

The relation between the steering angle of the front wheels,  $\lambda_1$ , and the measured steering wheel angle,  $\beta_v$ , and steering system ratio,  $i_u$ , is as follows:

$$\lambda_1 = \frac{\beta_v}{i_u} \quad (26)$$

Developed mathematical model in figure 2 enables simulation of different output values:

- $\ddot{\varepsilon}$ ,  $\dot{\varepsilon}$ ,  $\varepsilon$  - vehicle angular vibrations around the vertical gravity axis,

- $\dot{\theta}, \theta$  - body slip angular vibrations,
- $\delta_1, \delta_2$  - side slip angles of the front and the rear tires, respectively,
- $Y_1, Y_2$  - lateral forces on the front and the rear wheels, respectively,
- $\ddot{y}$  - lateral acceleration at vehicle suspended mass centre of gravity and
- $Y_{in}$  - lateral component of inertial force at the vehicle's centre of gravity.

### 3. Results of simulation of lateral vehicle dynamics

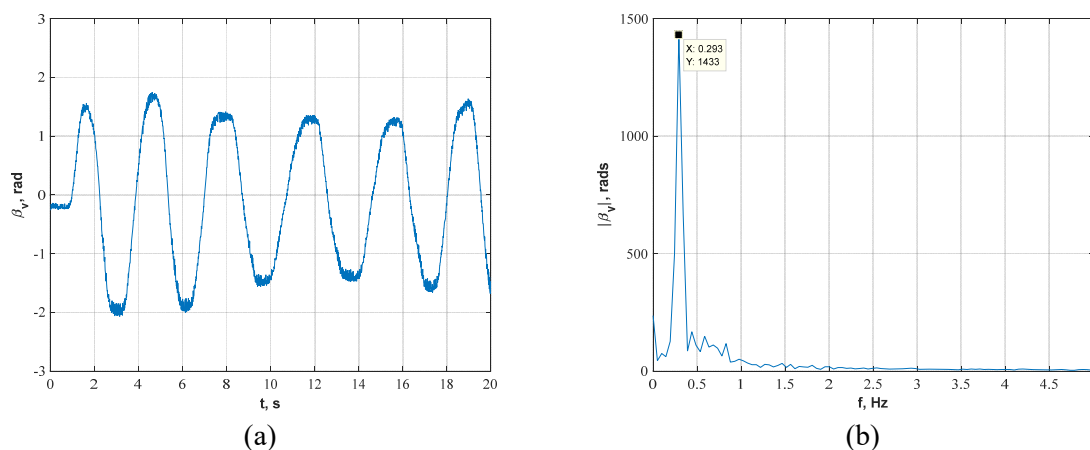
Simulations were conducted for a passenger vehicle with parameters given in table 1.

**Table 1.** Vehicle parameters [10].

Parameter, unit	Value
$m$ , kg	1090
$J_z$ , kg · m <sup>2</sup>	2000
$a$ , m	1.4
$b$ , m	1.1
$k_1$ , N · rad <sup>-1</sup>	44500
$k_2$ , N · rad <sup>-1</sup>	56500
$i_u$ , —	17.4

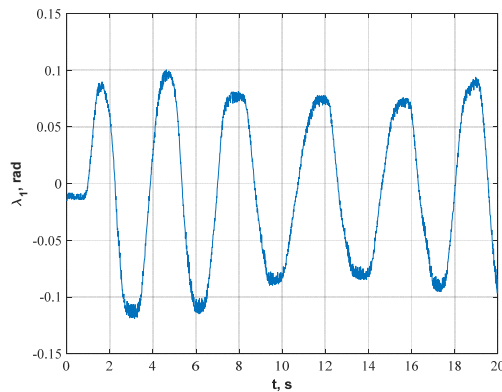
Figures 3 to 11 present simulation inputs and outputs for vehicle motion with variable speed over asphalt in good condition. During experiment, the driver was asked to turn the steering wheel according to harmonic low.

Figure 3 (a) shows the recorded values of the steering wheel angle,  $\beta_v$ . The driver has, basically, achieved a quasiharmonic function of the steering wheel angle, with dominant frequency of 0.293 Hz, that is visible in diagram of spectrum intensity of the steering wheel angle shown in figure 3 (b).



**Figure 3.** Steering wheel angle: (a) in time domain, (b) in spectral domain.

Steer angle of the front wheels,  $\lambda_1$ , was calculated as an input, according to equation (26) and presented in figure 4. Longitudinal velocity of the vehicle,  $v_x$ , recorded during experiment is presented in figure 5. Vehicle's velocity was variable, with periods of vehicle accelerating and decelerating, inducing nonstationary behavior.



**Figure 4.** Steer angle of the front wheels,  $\lambda_1$ .

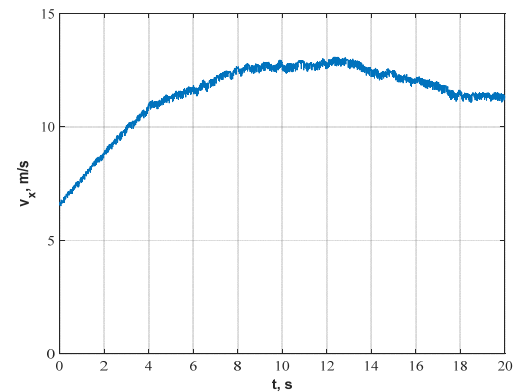


**Figure 5.** Longitudinal vehicle velocity,  $v_x$ .

As results of vehicle's lateral dynamics simulation using the adopted model, angular vibrations of the vehicle around the vertical axis (yaw angle,  $\varepsilon$ ) were presented in figure 6. It may be seen that the curve presented in figure 6 has a wave character which corresponds to the model's basic excitation - steer angle of the front wheels,  $\lambda_1$ .

Figure 7 presents vehicle body slip angle,  $\theta$ . Angular body slip vibration has also the wave shape that corresponds to model excitation in the form of quasiharmonic function of  $\lambda_1$ . Maximal values of body slip angle  $\theta$  are found in the area of  $\pm 1.4^\circ$ .

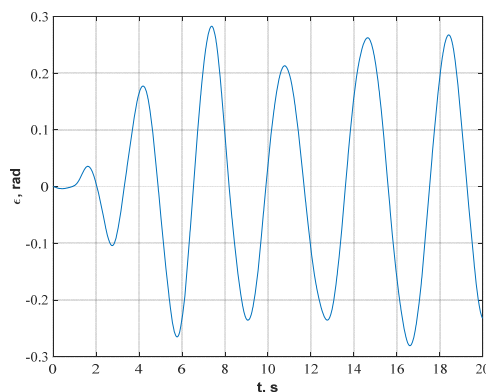


**Figure 6.** Angular vibrations of the vehicle around the vertical vehicle axis,  $\varepsilon$ .

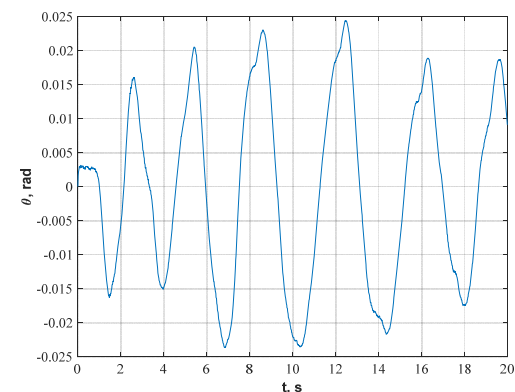


**Figure 7** Body side slip angular vibrations,  $\theta$ .

Values of tire side slip angles obtained by simulation of vehicles lateral dynamic are shown in figure 8. The front tire side slip angle is presented in figure 8 (a), while the rear tire side slip angle is presented in figure 8 (b). It may be seen that values of side slip angles are less than  $4^\circ$ , so the use of linear relationship between the tire side slip angles and corresponding lateral dynamic reactions on the wheels is justified.

Results of simulation of lateral dynamic reaction on the front wheels,  $Y_1$ , are shown in figure 9 (a), while those of lateral dynamic reaction on the rear wheels,  $Y_2$ , are shown in figure 9 (b). Values of the lateral dynamic reaction on the rear wheels are greater than corresponding values on the front wheels. This is due to the position of the vehicle's center of gravity, which is more distant from the front axle than from the rear axle ( $a > b$ ). For this reason, the portion of the lateral inertial force that is distributed to the rear axle is bigger than that distributed to the front axle.



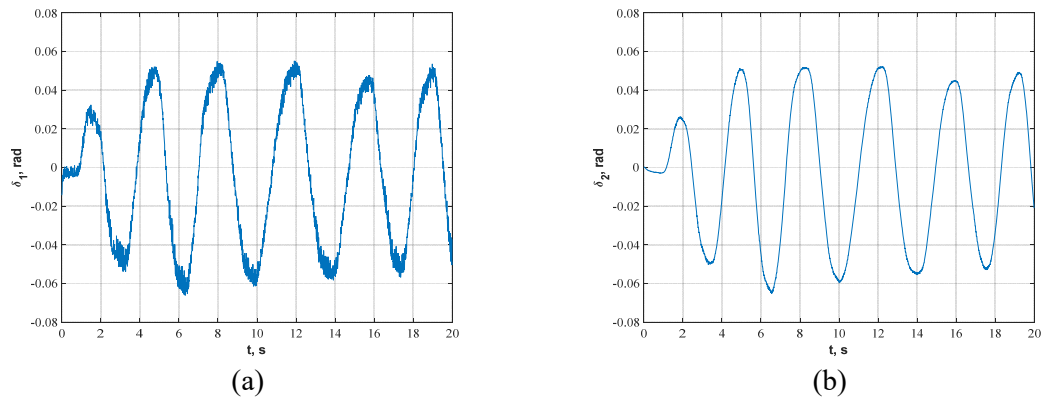


**Figure 8.** Side slip angles of: (a) the front wheels, (b) the rear wheels.

Angular rotation of the wheels induces the vehicle lateral acceleration,  $\ddot{y}$ , shown in figure 10. This acceleration has a trend that corresponds to given input - steer angle of the front wheels,  $\lambda_1$ .

The resulting lateral inertial force is shown in figure 11. It may be seen that this force is approximately equal to the sum of lateral reactions on the front and the rear wheels, because, due to small values, the influence of the front wheels steer angle,  $\lambda_1$ , is practically negligible.

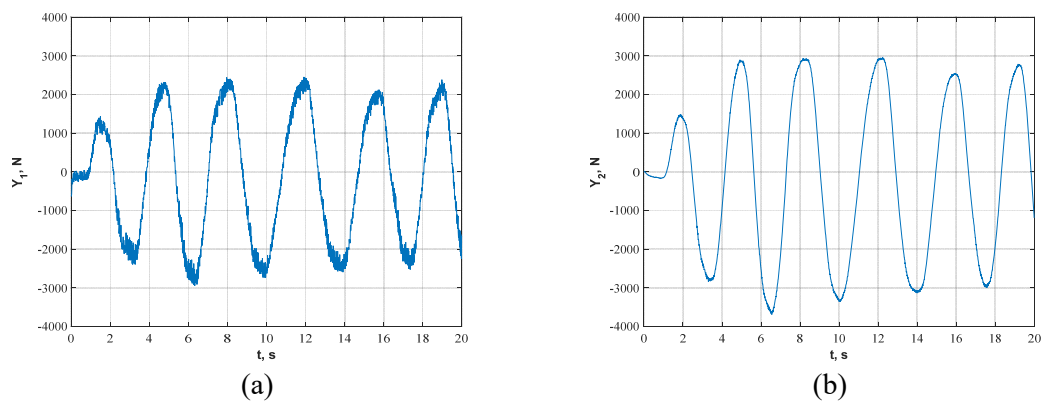


**Figure 9.** Lateral dynamic reactions: (a) on the front wheels, (b) on the rear wheels.

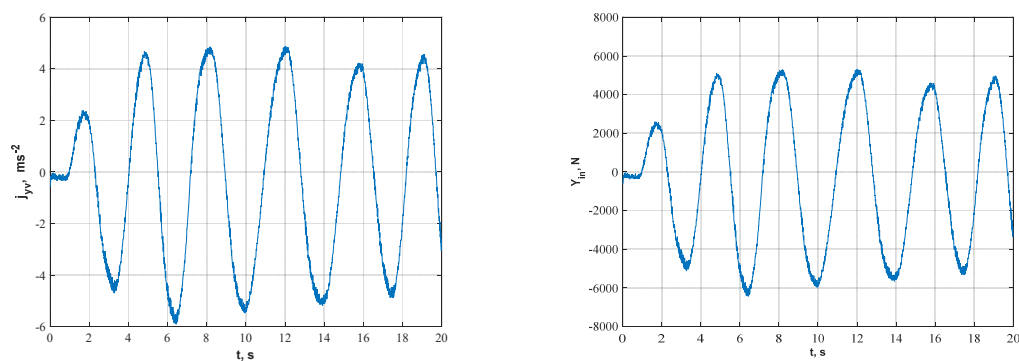


**Figure 10.** Vehicle's lateral acceleration.

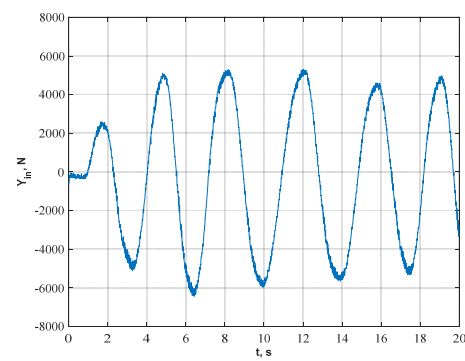


**Figure 11.** Vehicle's lateral inertial force.

#### 4. Conclusions

Linear single-track models of vehicle lateral dynamics can help in understanding the vehicle handling behavior, especially during stationary ride. However, in order to analyze the nonlinear phenomena in

lateral vehicle dynamics during nonstationary ride, nonlinear nonstationary single-track models ought to be used.

The developed nonlinear model of vehicle lateral dynamics was used for simulation with real, experimentally obtained inputs – variable: vehicle longitudinal velocity and steering wheel angle in the form of quasiharmonic curve. Model offers simulation results for several output variables that are important for understanding the vehicle lateral dynamics. The obtained results show that all output curves have a wave character which corresponds to the model's basic excitation - steer angle of the front wheels. In addition, all simulated curves have the same dominant frequency as the input curve of the front wheel steer angle. The influence of variable velocity and system nonlinearities can not be clearly seen in the time domain, so further analysis in spectral domain is necessary.

Acquired experimental data and the developed single-track model of the vehicle lateral dynamics may serve as a basis for application of estimation techniques in system parameter identification and for solving the problem of optimal control with the aspect of estimation of lateral vehicle dynamics.

### Acknowledgment

Research presented in this paper was financially supported by the Ministry of education, science and technological development of the Republic of Serbia, grant number TR35041.

### References

- [1] Jankovic A 2008 *Car dynamics* (in Serbian), Faculty of Mechanical Engineering from Kragujevac
- [2] Li L and Wang, F Y 2007 *Advanced Motion Control and Sensing for Intelligent Vehicles*, Springer Science+Business Media, LLC
- [3] Schramm D, Hiller M and Bardini R 2014 *Vehicle Dynamics – Modeling and Simulation*, Springer-Verlag
- [4] Mitschke, M 2005 Das Einspurmodell von Riekert-Schunck, *ATZ - Automobiltech Zeitschrift* **107**(11) 1030-31
- [5] Jazar, R 2008 *Vehicle Dynamics: Theory and Applications*, Springer Science+Business Media, LLC, 2008
- [6] Wong, J Y 2001 *Theory of ground vehicles*, John Wiley & Sons, Inc.
- [7] Borner, M 2006 *Modellierung, Analyse und Simulation der Fahrzeugquerdynamik*, In book: Isermann R (Ed.) *Fahrdynamik-Regelung*, 3 47-79, Friedr. Vieweg & Sohn Verlag | GWV Fachverlage GmbH
- [8] Pacejka, H B 2006 *Tire and Vehicle Dynamics*, Butterworth-Heinemann
- [9] Rouillard, V and Sek, M A 2001 Simulation of non-stationary vehicle vibrations, *Proceedings of the Institution of Mechanical Engineers, Part D: Journal of Automobile Engineering* **215**(10), 1069–75
- [10] Miloradović, D 2012 *Research of mechanical and functional couplings of vehicle dynamics system from the aspect of required performance*, Faculty of Engineering of the University of Kragujevac, Serbia, Doctoral Thesis